Effect of Bioactivation on Traditional Surfaces and Zirconium Nitride: Adhesion and Proliferation of Preosteoblastic Cells and Bacteria

Effect of bioactivation on traditional surfaces and Zirconium Nitride: adhesion and proliferation of preosteoblastic cells and bacteria

Authors

*Roberto Pistilli[1]

*Tullio Genova[2,5]

Luigi Canullo[3]

Maria Giulia Faga[4]

Maria Elena Terlizzi[5]

Giorgio Gribaudo[5]

Federico Mussano[2]

*equally contributed

1. San Camillo Hospital, Rome, Italy
2. C.I.R Dental School, Department of Surgical Sciences, University of Turin, Turin, Italy
3. Private practice, Rome, Italy
4. National Council of Research CNR-IMAMOTER, Turin, Italy
5. Department of Life Science and System Biology, University of Turin, Turin, Italy

Corresponding Author

Luigi Canullo, Via Nizza, 46 – 00198 Rome, Italy

Phone +39 347 6201976

Email: luigicanullo@yahoo.com

Abstract

Background: The aim of the present in vitro study was to reproduce and evaluate the response of bone and bacteria to traditional and innovative implant surfaces with difference wettability.

Materials & methods: Two hundred fifty-two samples made of grade 4 titanium with different coating (machined, MAC; double etched, Ti-treated; Zirconium Nitride, Ti-ZrN) were used for this in vitro study. Disks were divided in test (bio-activated using Plasma of Argon) and control group (untreated).

To assess the surface morphology of the specimens, representative images were acquired recurring to a SEM. To characterize the biological response *in vitro*, the widely diffused pre-osteoblastic murine cell line MC3T3-E1 was used. To quantify the amount of protein adsorbed, the titanium disks were incubated in presence of Fetal Bovine Serum (FBS) in Phosphate Buffered Saline (PBS) at 2% concentration. The sterilized titanium disks were then colonized by bacterial species from a single sputum sample obtained from a healthy volunteer. For every analysis, 24 disks were used (12 for each group).

Results: Compared to control groups, plasma treatment significantly increase the protein adsorption level on all different titanium surfaces (5.88±0.21 vs 7.85±0.21, 7.13±0.14 vs 9.74±0.65, 4.41±0.62 vs 6.13±0.52 respectively for MAC, Ti- treated and Ti-ZrN). Similar behavior was descripted for cell adhesion (27.67±2.03 vs 58.00±20.13, 116.67±12.02 vs 159.33±8.09, 52.00±4.73 vs 78.33±4.67 respectively for MAC, TR and Ti-ZrN).

Plasma treatment significantly augmented the number of CFU only in MAC and ZrN samples.

Conclusions: With the limitations of the present in vitro study, the following conclusions could be drawn: a) rough implant surfaces present a higher adhesion and proliferation of preosteoblastic cells and bacterial biofilm; b) rough implant surfaces benefited the most by the Plasma of Argon treatment

Keywords: plasma of Argon, implant surfaces, cell adhesion, protein adsorption, microbiological growth, zirconium Nitride

Introduction

Peri-implantitis has been recently characterized as an emerging disease [1]. Although the etiology seems so far to be controversial, the most accepted hypothesis is represented by a bacterial contamination of the peri-implant sulcus [2]. Absence of transgingival fibers, with real sealing ability, accelerates bacterial progression to bone [3,4]. This microbiological event was described to trigger cytokines expression and osteoclasts activation with consequent clinically relevant bone destruction [5].

Different studies, however, highlighted the importance of the surface roughness in the onset and progression of microbiological adhesion, although some controversies still remain [6,7]. For this reason, to limit microbiologic adhesion to implant surface, use of smoother surfaces was suggested. However, long term studies highlighted that this micro-topography resulted in high failure rate in case of low density bone [8].

From a clinical perspective, mostly the collar portion was descripted to be the key factor in peri-implant bone resorption. For a long period, immediately after smooth surface Implants by Branemark System, hybrid implants with smooth collar and neck have been available on the market with good clinical outcomes [9].

In the last decade, increasing of peri-implant disease rate around fully treated surfaces motivated researcher to analyze new surface configuration, with the aim to minimize bacterial adhesion to the implant components [10]. In fact, physical surface treatments and the consequent surface roughness play a more relevant role than only chemical modifications [11–13].

To prevent bacterial adhesion to implant collar, hydrophobic coatings or low hydrophilic materials were suggested [14]. The use of zirconia in implant dentistry has rapidly expanded over the past decade, driven by its advantageous physical, biological and corrosion properties [15]. In fact, despite its lower osteoblast adhesion, it was demonstrated that this material may represent a material surface less attractive for early plaque retention compared to titanium [16,17].

At the same time, *in vivo* and *in vitro*, zirconium nitride coating was demonstrated to alter the microbial composition in the short- and in the long-term exposure [18]. Moreover, in a different in vitro study, zirconium nitride was shown to favor cellular attachment of human gingival fibroblast [19]. In addition, *in vitro*, zirconium nitride thin films were shown

to make the surface of the titanium more bioactive for preosteoblast cell than uncoated titanium surfaces [20]. Enhancement of physical surface properties (increasing surface energy and therefore hydrophilicity) was shown to positively affect early bone responses. In the last few years, application of plasma technology on titanium surfaces highlighted that this technology allows to reach a higher wettability and, therefore, a stronger cell adhesion [21,22].

In fact, plasma of Argon treatment at appropriate parameters was demonstrated to moderately enhance hydrophilicity positively charging surfaces: this may promote good adhesion levels.

The aim of the present in vitro study was to reproduce and evaluate the response of bone and bacteria to traditional and innovative implant surfaces with difference wettability. For this reason, the response of different surfaces [smooth and rough titanium (control) and zirconium nitride coated titanium (test)] to cells (pre-osteoblasts) and bacteria pre- and after plasma of Argon treatment was measured.

Materials and methods

Sample preparation

Two hundred fifty-two samples made of grade 4 titanium (Resista, Omegna (VB), Italy) were machined to obtain 8 mm × 3 mm cylinders. Three different surfaces were attained. Machined titanium was used in the following to refer to the uncoated samples (Ti MAC). Rough surfaces were prepared starting from pristine titanium by dual acid etching (Ti-AE). Zirconium nitride thin film coating (henceforth named Ti-ZrN) was grown on pristine Titanium by radio frequency - plasma enhanced chemical vapor deposition (RF-PECVD).

Sample size

A priori power analysis was prepared, referring to similar in vitro trials. If the true difference in the experimental and control means is 1.548, the study sample size will be represented by 12 experimental subjects and 12 control subjects to be able to reject the null hypothesis that the population means of the experimental and control groups are equal with probability (power) 0.95. The Type I error probability associated with this test of this null hypothesis was set at 0.05.

Twelve disks for each surface modifications (sub-groups) were randomly allocated into one of the 2 treatment groups (Argon plasma versus no treatment) according to a computer-generated randomization list prepared in advance by an external investigator, not involved in the study, who was aware of the sequence and could have access to the file. (Fig. 1).

Scanning Electron Microscopy

To assess the surface morphology of the specimens, representative images were acquired recurring to a Scanning Electron Microscope (Zeiss EVO 50, Carl Zeiss AG, Oberkochen, Germany). Implants were cleaned in an acetone ultrasonic bath for 10 min, immersed in isopropanol for 10 min, then rinsed in deionized water and finally dried prior to be analyzed. Sterile forceps were used to avoid contamination.

Roughness analysis

Area surface roughness parameters [23] at different sites of the implant were obtained by scanning electron microscope, using an EVO MA 10 SEM (Zeiss).

In particular, the Stereo-SEM (SSEM) technique was used. This approach exploits the basic principle of stereo vision to turn conventional SEM images into three-dimensional surface topography reconstructions. Basically, two images of the same field of view are acquired after eucentric rotation by a given angle. This is obtained by changing the angle between the sample and the electrons source, by tilting the table bearing the sample. The tilting angle is set and controlled by the instrument control software. The couple of images obtained (stereopair), the size of the field of view and the tilting angle are the incoming data, that are processed by a specific software (Mex 6.0, Alicona Imaging).

Three-dimensional images obtained by this process allows to measure height profiles or areas, and to calculate the different roughness parameters defined by relevant literature and standards.

In the present analysis, SEM images used to build-up stereo-pairs were obtained at 2000 x. Roughness parameters according to ISO25178 were obtained from reconstructed images of 80 x 110 micrometers area

Cell adhesion

Among the different osteoblast and pre-osteoblast cell model available [24–26], the widely diffused pre-osteoblastic murine cell line MC3T3-E1 (ECACC, Salisbury, UK) was used to characterize the biological response *in vitro* [24]. Cells were maintained in Alpha MEM supplemented with 10% fetal bovine serum (Life Technologies, Milan, Italy), 100 U/ml penicillin, 100 mg/ml streptomycin, were passaged at subconfluency to prevent contact inhibition and were kept under a humidified atmosphere of 5% CO_2 in air, at 37°C.

Cell adhesion was evaluated on titanium samples using a 48-well plate (BD, Milan Italy). Cells were detached using trypsin for 3 minutes, carefully counted and seeded at 3×10^3 cells/well in 100 µl of growth medium on the different samples. The 48-well plates were kept at 37 °C, 0.5 % CO_2 for 20 min. Before and after fixation in 4% paraformaldehyde in PBS for 15 min at room temperature, cells were washed two times with PBS and then stained with 1µM DAPI (Molecular Probes, Eugene, California, USA) for 15' at 37°C to stain cell nuclei. Images were acquired using a Nikon Eclipse T-E microscope [27,28]. Cell nuclei were counted using the 'Analyze particles' tool of ImageJ

software (ImageJ, U. S. National Institutes of Health, Bethesda, Maryland, USA, http://imagej.nih.gov/ij/) [29,30].

Protein adsorption

As reported elsewhere [31], to quantify the amount of protein adsorbed, the titanium disks were incubated in presence of Fetal Bovine Serum (FBS) in Phosphate Buffered Saline (PBS) at 2% concentration, at 37°C for 30 minutes. Subsequently, the samples were washed twice with PBS and the adsorbed protein was eluted from the disks using RIPA buffer for 10 minutes [32]. Total protein amount was quantified using SERVA BCA Protein Assay Micro Kit (SERVA Electrophoresis GmbH, Heidelberg, Germany) following the manufacturer's instructions.

Bacterial biofilm evaluation

The sterilized titanium disks have been colonized by bacterial species from a single sputum sample obtained from one healthy volunteer. Bacteria were grown over night in 10mL of Mueller Hinton (MH) broth (Sigma Aldrich) at 37°C. The day after, bacteria were subcultured until a spectrophotometric density of 0.6 at 600nm was reached, corresponding to 1×10^8 colony forming units/mL (CFU/mL), approximately. Each disc was incubated with 1mL of MH broth (for negative control) or 1mL of bacterial suspension in a 24-well plate by using a shaking rotator (80rpm) at 37°C for 24h. Non-adherent bacteria were removed by rinsing each disk in sterile saline, followed by 10 seconds of vortex for 6 times. Discs were then transferred into a sterile plastic container with 1mL saline solution and immersed in ultrasonic bath at 80 kHz with a power output of 250W [33]. After sonication, 10-fold dilutions of each supernatant were incubated in MH plate for colonies counting.

Statistical analysis

Data were analyzed by GraphPad Prism6 (GraphPad Software, Inc., La Jolla, CA, USA). Each experiment was repeated at least three times. Statistical analysis was performed by using ANOVA. A p value of <0.05 was considered significant.

Results

Topography

The three surfaces tested are depicted in figure 2. Machined (Ti MAC) samples display the typical marks of the milling process (Fig. 2A, B), which are still recognizable in the ZrN thin film coated samples (Fig. 2E, F). On the other hand, Ti-AE (Fig. 2C, D) disks appeared as a typical roughened surface, as it could be anticipated for the product of dual acid etching treatment.

Surface roughness

Representative images of the different sites of the implant are shown in fig. a (machined), and b (roughened). Fig. c and d show three dimensional pseudo-colour depth images of the same areas. Area roughness parameters obtained from the images are reported in Table 1.

Protein adsorption

As shown in figure 3 and resumed in Tab 2, plasma treatment significantly increased the protein adsorption level on all titanium surfaces. Moreover, Ti-AE samples significantly increased the level of protein adsorption (7.13 vs 9.74) compared to Ti MAC (5.88 vs 7.85) and Ti-ZrN (4.41 vs 6.13) (p-value: 0,0286).

On the other hand, Ti-ZrN surface did not show significant difference compared to Ti MAC (p-value: 0,0571).

Early response of osteoblasts

As depicted in figure 4 and resumed in Tab 3, on all different titanium surfaces, plasma treatment significantly enhanced the cell adhesion level. Interestingly, both Ti-AE (116.67 vs 159.33) and Ti-ZrN (52.00 vs 78.33) samples significantly increased the MC3T3-E1 adhesion compared to Ti MAC (27.67 vs 58.00) (pvalue:0.010). Moreover, Ti treated samples strongly improved cell adhesion also compared to Ti-ZrN (0.0142).

Bacterial growth

In order to understand how plasma treatment of different Ti surfaces may affect bacterial growth, biofilm formation was evaluated at 24 h recurring to CFU count. As reported in figure 5 and resumed in Tab. 4, plasma treatment significantly augmented the number of CFU only in Ti MAC (1.111^5 vs 2.139^5) and Ti ZrN (1.339^5 vs 2.017^5) samples, but not in TI-AE (2.767^5 vs 2.278^5). On the other hand, in the control group, Ti-AE samples presented significantly higher bacterial growth compared to Ti MAC and Ti-ZrN samples (pvalue:0,0167).

Absence of differences in the EI-AE group after plasma treatment might be due to a saturation effect.

Discussion

The present in-vitro study investigated the effect of bio-activation through plasma of Argon on different implant surfaces. All activated surfaces demonstrated an increased affinity to cells and proteins involved in osseointegration (protein adsorption and osteoblast-like cells adhesion), but also to bacteria.

Although implant supported rehabilitations were described to have a minimal failure rate, in critical anatomical (elderly people, patients with altered osseointegration processes) or surgical (immediate loading, implants inserted in grafted sites, short implants, low quality or quantity of bone) conditions, implants might present an increased failure rate [34–36].

In these conditions, a more reactive surface would be helpful, increasing BIC and ensuring a faster and stronger osseointegration. Research was highly focused on this field, developing the so called "osseoconductive" surfaces [37].

However, reports of increasing peri-implant disease incidence around fully etched-, HA-, or TPS-treated implants might suggest that a osseoconductive surface near the implant-abutment connection could might be more prone to biologic complications following bacterial biofilm growth, if compared to smooth surfaced.

To prevent any possible microbiologic disadvantages and exploit osseoconductive properties, hybrid surfaced implants were brought on the market. This generation of implants were designed, in fact, with a rough surface in the apical portion of the fixture and a smooth collar. The positive experience reported by machined and microtextured surfaces influenced the development of alternative surfaces, ideally capable to minimize bacterial adhesion, including Zirconium Nitride [38,39].

Although surfaces repellent for bacteria were supposed to decrease affinity also for bone regenerative cells, Zirconium Nitride coating was demonstrated to be bioactive compared to smooth titanium [20]. In the present study, protein adsorption tests demonstrated that smooth surface behaved slightly better compared to Zr-Ni coating. On the other hand, this material showed a slightly higher cell adhesion if compared to smooth titanium disks. Obviously, the dual acid etched surface presented significantly better outcomes in terms of cell adhesion and protein

adsorption. This behavior seems to be correlated to the higher contact area available to cells and proteins.

Analyzing microbiological outcomes, focusing on the control conditions (Ti MAC), data reported an increase of biofilm on rough surface which is significantly higher compared to smooth surface and zirconium nitride. This is in accordance with the already published literature, which reports how these surfaces demonstrated less microbiological affinity compared to rougher micro-geographies [18,19].

While a bio-activation treatment might increase the titanium reactivity to bone environment, on the other hand, it seems to increase also the affinity to bacterial biofilm. In the present study, in fact, plasma treatment increased more than 2 times the bacterial growth on machined disks and almost 1.5 on Zirconium Nitride. Surprisingly, bio-activation, decreased the bacterial growth on the studied rough surface. However, this might be due to a saturation effect. Additionally, large standard deviation values might suggest that microbiological contamination values should be interpreted with caution.

In fact, while intergroup comparison demonstrated significant differences in the control condition with slightly better performance of machined and Zirconium Nitride surfaces, this difference disappeared when analyzing the intergroup comparison at the test conditions, although Zirconium Nitride presented a slightly better outcome.

However, the phenomenon might be clinically irrelevant. In fact, these surfaces were ideally created to be in contact at the time of the implant insertion with bone or connective tissues. Only an incorrect implant positioning might expose surfaces to the contaminated oral environment. Additionally, it must be highlighted that bio-activation through plasma of Argon has a time-dependent effect. As demonstrated by Canullo et al. [40], the favorable influence of this treatment dramatically decreases in 48h. While it represents a control factor, this seems to be clinically relevant during the soft- and hard-tissue healing processes and the physiological protein cascade which are maximum in the first 48 hours [41].

However, data described in the present study might recommend the clinical advantage of a hybrid surfaced implant (apical portion with a titanium rough surface to increase osseointegration and coronal portion with smooth surface or

Zirconium Nitride coating). At the same time, positive outcomes reported in the test group might suggest that plasma of Argon treatment could exploit this hybrid surface configuration.

To better simulate clinical conditions and better generalize the clinical relevance, low concentrations of factors involved in the osseointegration process (proteins in Bovine Fetal Serum and murine pre-osteoblasts) were used in the present in vitro study. In fact, based on previous experiments [21,30,42,43], higher numbers of cells or protein amounts were found to conceal the effect of plasma of Argon, due to a saturation effect [40].

To explain results with statistically significant increase of protein, cells and bacteria after test conditions, biophysical effect of plasma treatment on Titanium surfaces should be clearly declared. Bio-activation though plasma of Argon, in fact, activates the electronic mantle of the external surface. This phenomenon produces an increasing surface energy and therefore hydrophilicity [30]. Obviously, this activated status reflects on cell or protein interaction with Titanium. Being similar biologic adhesion cascade, similar influence was proven to be active also on bacteria.

Although this study is only in vitro and it represents just a preliminary overview on the topic, the data obtained encourage the design and execution of clinical trials, in absence of which the relevance of the reported outcomes should be interpreted with caution.

Conclusions

With the limitations of the present in vitro study, the following conclusions could be drawn:

1. Rough implant surfaces present a higher adhesion and proliferation of preosteoblastic cells and bacterial biofilm.
2. Rough implant surfaces benefited the most by the Plasma of Argon treatment.

Acknowledgements

All authors explicitly declare that they have no conflict of interest.

Authors are grateful to Dr Cassinelli and Morra for their help in measuring surface roughness.

Tables

Table 1 *Area roughness parameters at different sites of the implant. All data are expressed as micrometers (μm) except for Sdr, wich is a % value. The different nature of surface roughness between the two sites is best shown by average vertical roughness values (Sa and Sq), which is nearly twofold on the roughened portion of the implant. Most important, the lateral roughness parameter Sdr, that is the ratio between the actual surface area and the geometrical area (in the present case, 110 x 80 micrometers) is 51.24% in the roughened portion and 28.12% in the machined one. Obviously, the microrough topography obtained on acid etching provides a very significant increase of the implant surface area.*

Parameter	Machined	Roughened	Description
Sa	0.34	0.62	Average height of selected area
Sq	0.43	0.77	Root-Mean-Square height of selected area
Sp	3.37	3.49	Maximum peak height of selected area
Sv	3.98	2.84	Maximum valley depth of selected area
Sz	7.35	6.32	Maximum height of selected area
Sdr	28.12	51.24	Developed interfacial area ratio

Table 2 *Numerical data pertaining to μg of protein per sample is reported as Mean and Standard Error*

Table 2: protein adsorption						
	Ti MAC CTRL	Ti MAC PLASMA	Ti-AE CTRL	Ti-AE PLASMA	Ti- ZrN CTRL	Ti ZrN PLASMA
Mean	5.88	7.85	7.13	9.74	4.41	6.13
SE	0.21	0.21	0.14	0.65	0.62	0.52

Table 3 *Numerical data pertaining to the number of cells adherent at 20 minutes is reported as Mean and Standard Error*

Table 3: cell adhesion						
	Ti MAC CTRL	Ti MAC PLASMA	Ti-AE CTRL	Ti-AE PLASMA	Ti- ZrN CTRL	Ti ZrN PLASMA
Mean	27.67	58.00	116.67	159.33	52.00	78.33
SE	2.03	20.13	12.02	8.09	4.73	4.67

Table 4 *Numerical data pertaining to CFU count is reported as Mean and Standard Error*

Table 4: microbiological contamination (CFU)						
	Ti MAC CTRL	Ti MAC PLASMA	Ti-AE CTRL	Ti-AE PLASMA	Ti-ZrN CTRL	Ti-ZrN PLASMA
Mean	1.111E+05	2.139E+05	2.767E+05	2.278E+05	1.339E+05	2.017E+05
SE	1.198E+04	3.530E+04	4.554E+04	2.333E+04	2.878E+04	2.151E+04

Figures

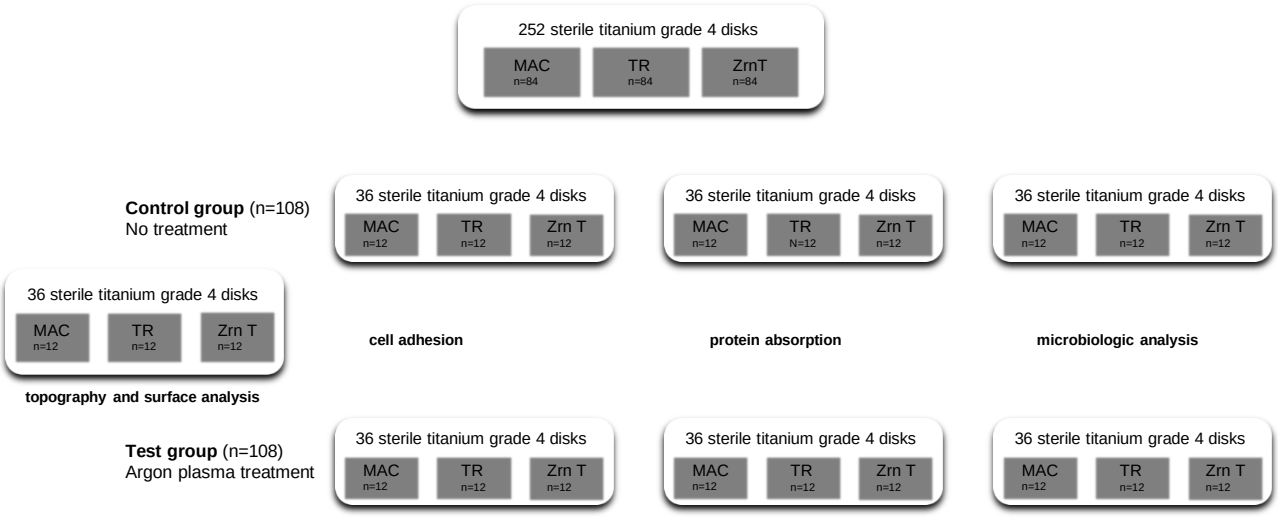

Figure 1: flow chart of the experiment

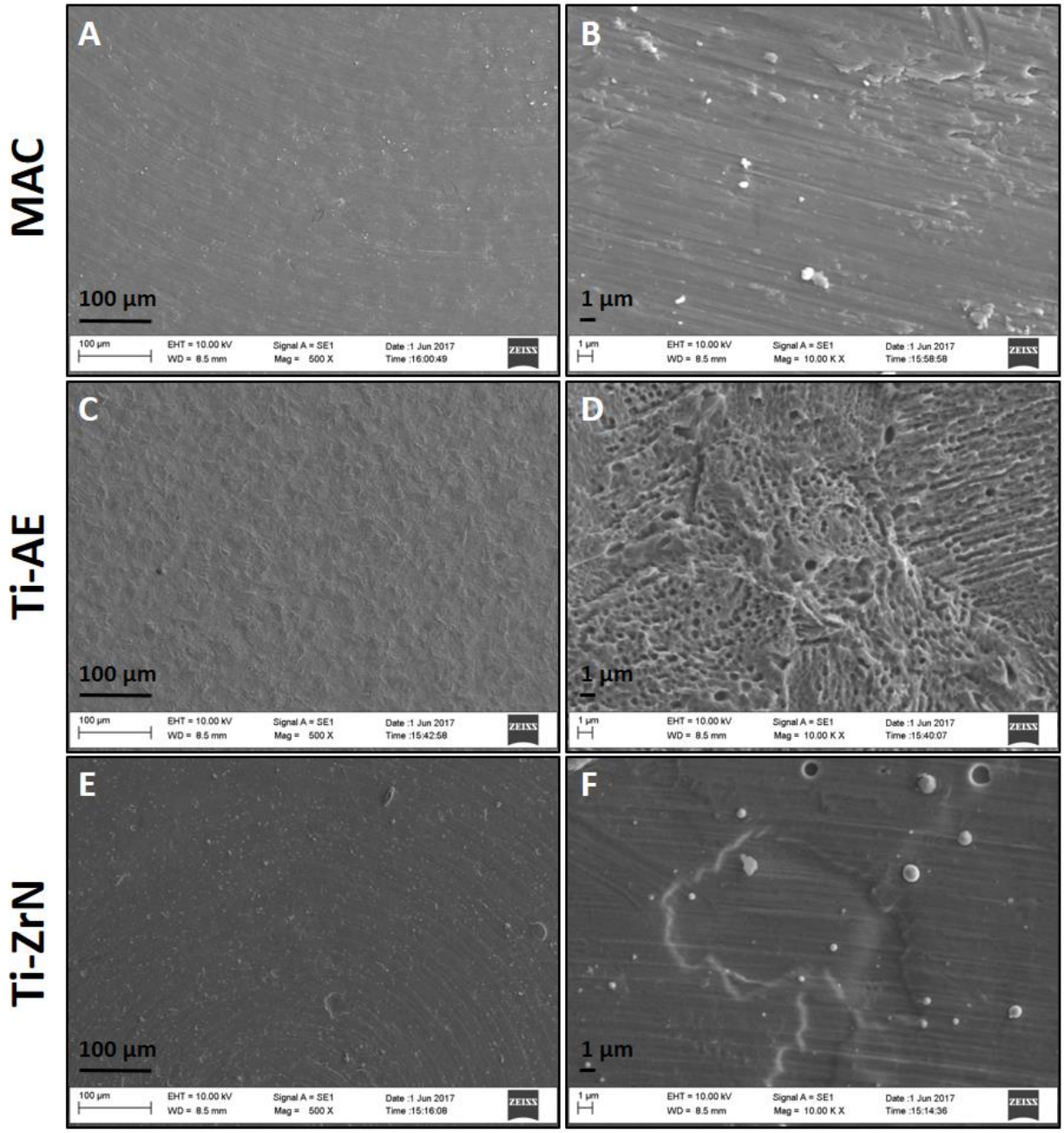

Figure 2: tested surfaces at SEM at 500x (a, c, e) and 10000x (b, d, f). a,b: Machined (Ti MAC) samples display the typical marks of the milling process. c, d: typical roughened dual etched surface. e, f: marks recognisable on ZrN thin film coated samples

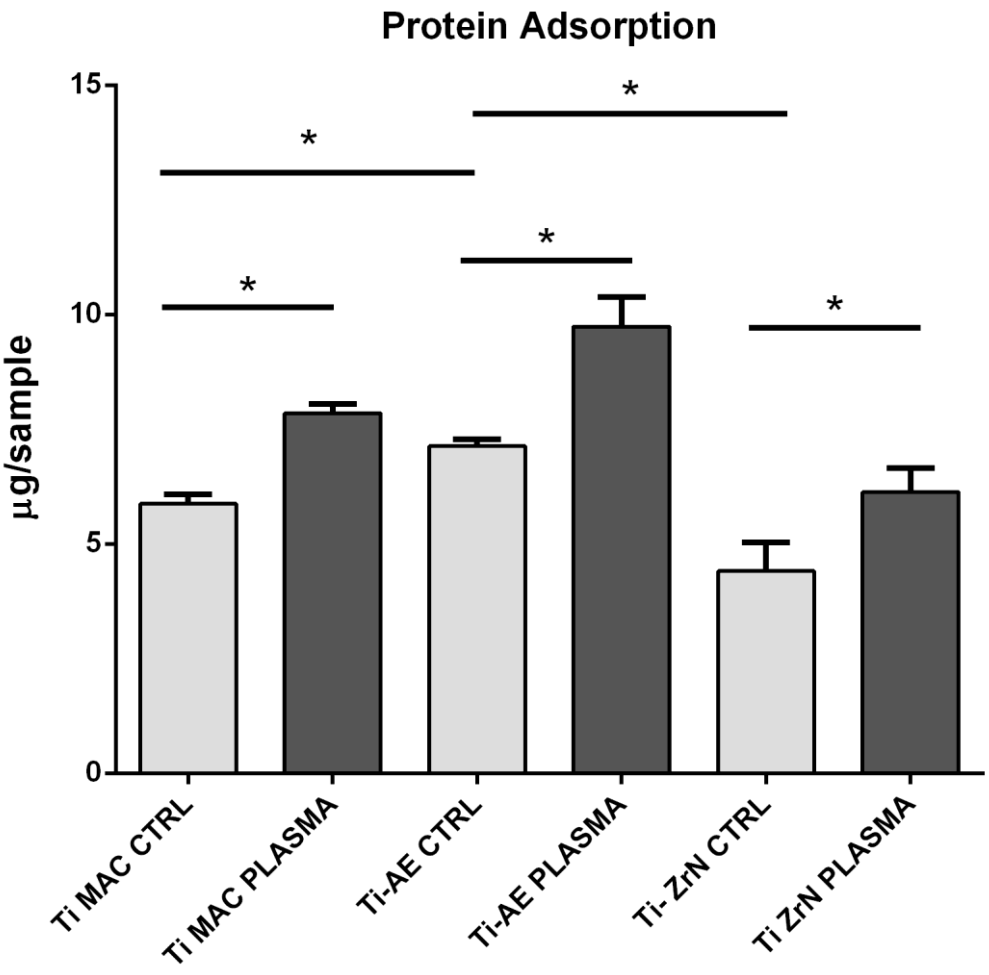

Figure 3. Protein adsorption assay performed incubating samples with 2% FBS in PBS for 30 minutes at 37C°. Values represents mean ± Standard Error; the symbol (*) indicates a statistically significant difference, considering a p-value < 0.05.

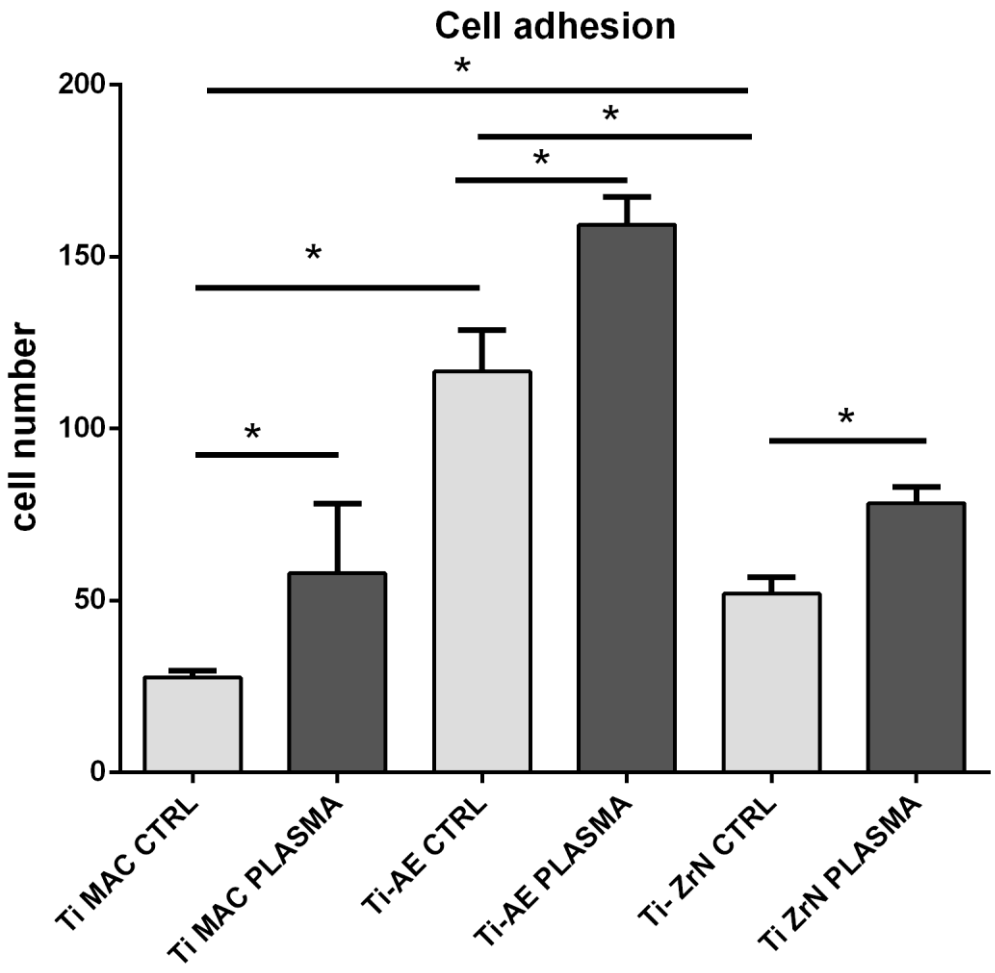

Figure 4. *Cell adhesion. MC3T3-E1 adhesion was evaluated on all samples at 20 min. The level of cell adhesion was measured counting the number of adherent cells for each field. Values represents mean ± Standard Error; the symbol (*) indicates a statistically significant difference, considering a p-value < 0.05.*

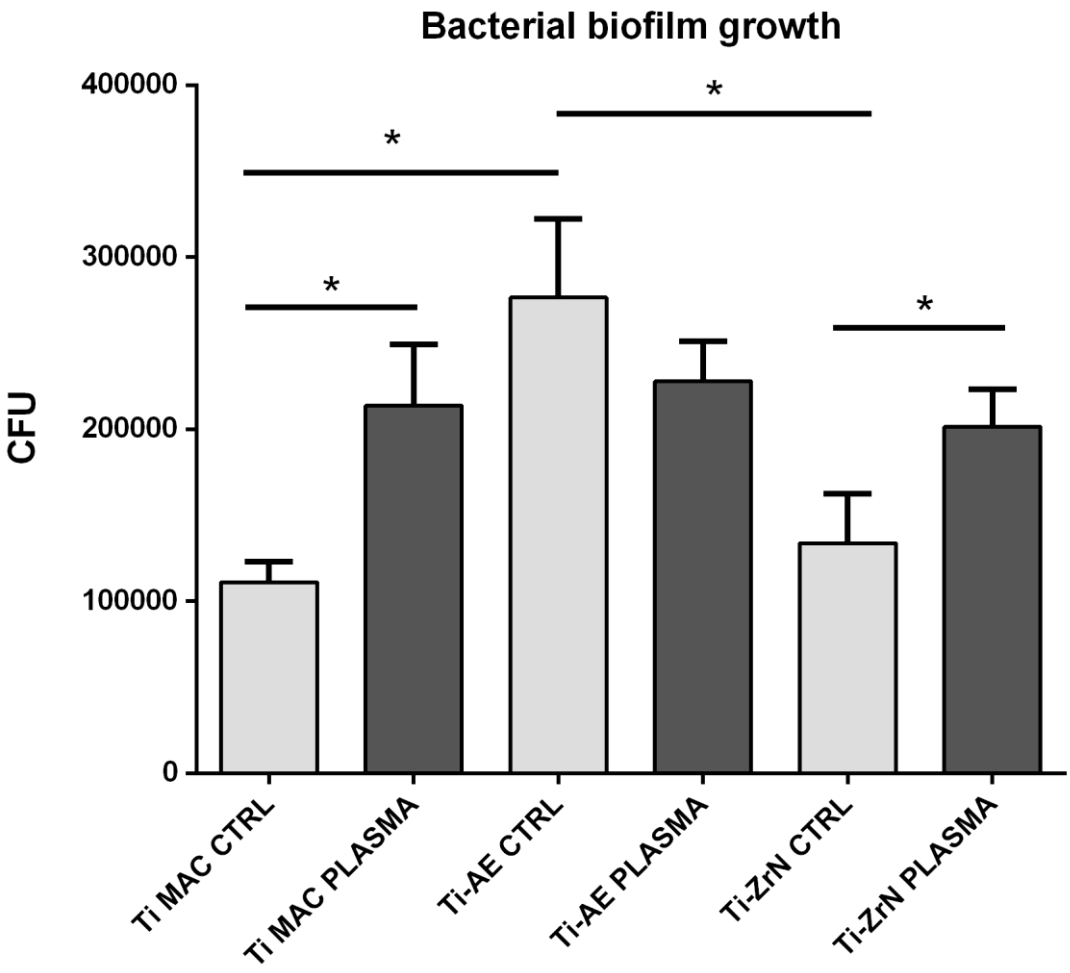

Figure 5. Evaluation of CFU of bacterial biofilm growth on Ti disks incubated in 1mL of bacterial suspension for 24h at 37C° in shaking. Values represents mean ± Standard Error; the symbol (*) indicates a statistically significant difference, considering a p-value < 0.05.

1. Lee, C.-T., Huang, Y.-W., Zhu, L. & Weltman, R. Prevalences of peri-implantitis and peri-implant mucositis: systematic review and meta-analysis. *J. Dent.* **62,** 1–12 (2017).

2. Paul Rosen, Donald Clem, David Cochran, S. F. Academy Report: Peri-Implant Mucositis and Peri-Implantitis: A Current Understanding of Their Diagnoses and Clinical Implications. *J. Periodontol.* **84,** 436–443 (2013).

3. Mussano, F. *et al.* Apical periodontitis: preliminary assessment of microbiota by 16S rRNA high throughput amplicon target sequencing. *BMC Oral Health* **18,** 55 (2018).

4. Bauman, G. R., Rapley, J. W., Hallmon, W. W. & Mills, M. The peri-implant sulcus. *Int. J. Oral Maxillofac. Implants* **8,** 273–280 (1993).

5. Dereka, X., Mardas, N., Chin, S., Petrie, A. & Donos, N. A systematic review on the association between genetic predisposition and dental implant biological complications. *Clinical Oral Implants Research* **23,** 775–788 (2012).

6. Albouy, J. P., Abrahamsson, I., Persson, L. G. & Berglundh, T. Spontaneous progression of peri-implantitis at different types of implants. An experimental study in dogs. I: Clinical and radiographic observations. *Clin. Oral Implants Res.* **19,** 997–1002 (2008).

7. Albouy, J. P., Abrahamsson, I. & Berglundh, T. Spontaneous progression of experimental peri-implantitis at implants with different surface characteristics: An experimental study in dogs. *J. Clin. Periodontol.* **39,** 182–187 (2012).

8. Jaffin, R. A. & Berman, C. L. The Excessive Loss of Branemark Fixtures in Type IV Bone: A 5-Year Analysis. *J. Periodontol.* **62,** 2–4 (1991).

9. Browaeys, H. *et al.* A retrospective analysis of early and immediately loaded osseotite implants in cross-arch rehabilitations in edentulous maxillas and mandibles up to 7 Years. *Clin. Implant Dent. Relat. Res.* **15,** 380–389 (2013).

10. Derks, J. *et al.* Effectiveness of implant therapy analyzed in a Swedish population: early and late implant loss. *J. Dent. Res.* **94,** 44S–51S (2015).

11. Mussano, F. *et al.* Nano-Pore Size of Alumina Affects Osteoblastic Response. *Int. J. Mol. Sci.* **19,** 528 (2018).

12. Mussano F, Genova T, Laurenti M, Zicola E, Munaron L, Rivolo P, Mandracci P, C. S. Early response of fibroblasts and epithelial cells to pink-shaded anodized dental implant abutments: an in vitro study. *Int. J. Oral Maxillofac. Implants* (2018).

13. Vallée, A. *et al.* Alumina-zirconia composites functionalized with laminin-1 and laminin-5 for dentistry: effect of protein adsorption on cellular response. *Colloids Surf. B. Biointerfaces* **114,** 284–93 (2014).

14. Mussano, F. *et al.* Hydrogenated amorphous silicon coatings may modulate gingival cell response. *Appl. Surf. Sci.* **436,** 603–612 (2018).

15. Bosshardt, D. D., Chappuis, V. & Buser, D. Osseointegration of titanium, titanium alloy and zirconia dental implants: current knowledge and open questions. *Periodontology 2000* **73,** 22–40 (2017).

16. Hisbergues, M., Vendeville, S. & Vendeville, P. Review zirconia: Established facts and perspectives for a biomaterial in dental implantology. *Journal of Biomedical Materials Research - Part B Applied Biomaterials* **88,** 519–529 (2009).

17. Schierano, G. *et al.* An Alumina Toughened Zirconia Composite for Dental Implant Application: In Vivo Animal Results. *Biomed Res. Int.* **2015,** 1–9 (2015).

18. Größner-Schreiber, B. *et al.* Modified implant surfaces show different biofilm compositions under in vivo conditions. *Clin. Oral Implants Res.* **20,** 817–826 (2009).

19. Größner-Schreiber, B. *et al.* Focal adhesion contact formation by fibroblasts cultured on surface-modified dental implants: An in vitro study. *Clin. Oral Implants Res.* **17,** 736–745 (2006).

20. Rizzi, M. *et al.* Effect of zirconium nitride physical vapor deposition coating on preosteoblast cell adhesion and proliferation onto titanium screws. *J. Prosthet. Dent.* **112,** 1103–1110 (2014).

21. Canullo, L. *et al.* Plasma of Argon Affects the Earliest Biological Response of Different Implant Surfaces. *J. Dent. Res.* **95,** 566–573 (2016).

22. Mussano, F. *et al.* In vitro characterization of two different atmospheric plasma jet chemical functionalizations of titanium surfaces. *Appl. Surf. Sci.* **409,** 314–324 (2017).

23. Wennerberg, A., Albrektsson, T. & Wennerberg A, A. T. Suggested guidelines for

the topographic evaluation of implant surfaces. *Int. J. Oral Maxillofac. Implants* **15,** 331–344 (2000).

24. Genova, T., Munaron, L., Carossa, S. & Mussano, F. Overcoming physical constraints in bone engineering: 'the importance of being vascularized'. *J. Biomater. Appl.* **30,** 940–951 (2016).

25. Mussano, F. *et al.* Cytokine, Chemokine, and Growth Factor Profile Characterization of Undifferentiated and Osteoinduced Human Adipose-Derived Stem Cells. *Stem Cells Int.* **2017,** 1–11 (2017).

26. Mussano, F. *et al.* Osteogenic Differentiation Modulates the Cytokine , Chemokine , and Growth Factor Profile of ASCs and SHED. *Int. J. Mol. Sci.* **19,** 1454 (2018).

27. Fiorio Pla, A. *et al.* Multiple Roles of Protein Kinase A in Arachidonic Acid-Mediated Ca2+ Entry and Tumor-Derived Human Endothelial Cell Migration. *Mol. Cancer Res.* **8,** 1466–1476 (2010).

28. Petrillo, S. *et al.* Heme accumulation in endothelial cells impairs angiogenesis by triggering paraptosis. *Cell Death Differ.* **25,** 573–588 (2018).

29. Genova, T. *et al.* TRPM8 inhibits endothelial cell migration via a non-channel function by trapping the small GTPase Rap1. *J. Cell Biol.* **216,** 2107–2130 (2017).

30. Canullo, L. *et al.* Morphometric Changes Induced by Cold Argon Plasma Treatment on Osteoblasts Grown on Different Dental Implant Surfaces. *Int. J. Periodontics Restorative Dent.* **37,** 541–548 (2017).

31. Mussano, F. *et al.* Role of surface finishing on the in vitro biological properties of a silicon nitride–titanium nitride (Si3N4–TiN) composite. *J. Mater. Sci.* **52,** 467–477 (2017).

32. Fiorio Pla, A. *et al.* Differential sensitivity of prostate tumor derived endothelial cells to sorafenib and sunitinib. *BMC Cancer* **14,** 939 (2014).

33. Bjerkan, G., Witsø, E. & Bergh, K. Sonication is superior to scraping for retrieval of bacteria in biofilm on titanium and steel surfaces in vitro. *Acta Orthop.* **80,** 245–50 (2009).

34. Friberg, B., Jemt, T. & Lekholm, U. Early failures in 4,641 consecutively placed Brånemark dental implants: a study from stage 1 surgery to the connection of

completed prostheses. *Int. J. Oral Maxillofac. Implants* **6,** 142–6 (1991).

35. Fiorellini, J. P., Martuscelli, G. & Weber, H. P. Longitudinal studies of implant systems. *Periodontol. 2000* **17,** 125–131 (1998).

36. Del Fabbro, M., Testori, T., Francetti, L. & Weinstein, R. Systematic review of survival rates for implants placed in the grafted maxillary sinus. *Int. J. Periodontics Restorative Dent.* **24,** 565–577 (2004).

37. Le Guéhennec, L., Soueidan, A., Layrolle, P. & Amouriq, Y. Surface treatments of titanium dental implants for rapid osseointegration. *Dent. Mater.* **23,** 844–54 (2007).

38. Zetterqvist, L. *et al.* A Prospective, Multicenter, Randomized-Controlled 5-Year Study of Hybrid and Fully Etched Implants for the Incidence of Peri-Implantitis. *J. Periodontol.* **81,** 493–501 (2010).

39. Spinato, S., Bernardello, F., Sassatelli, P. & Zaffe, D. Hybrid and fully-etched surface implants in periodontally healthy patients: A comparative retrospective study on marginal bone loss. *Clin. Implant Dent. Relat. Res.* **19,** 663–670 (2017).

40. Canullo, L., Cassinelli, C., Götz, W. & Tarnow, D. Plasma of argon accelerates murine fibroblast adhesion in early stages of titanium disk colonization. *Int. J. Oral Maxillofac. Implants* **28,** 957–62 (2013).

41. Susin, C. *et al.* Wound healing following surgical and regenerative periodontal therapy. *Periodontol. 2000* **68,** 83–98 (2015).

42. Canullo, L., Genova, T., Wang, H.-L., Carossa, S. & Mussano, F. Plasma of Argon Increases Cell Attachment and Bacterial Decontamination on Different Implant Surfaces. *Int. J. Oral Maxillofac. Implants* **32,** 1315–1323 (2017).

43. Canullo, L. *et al.* Plasma of argon enhances the adhesion of murine osteoblasts on different graft materials. *Ann. Anat. - Anat. Anzeiger* **218,** 265–270 (2018).